atmosphere

MDPI

Article

Temporal Variations of the Turbulence Profiles at the Sayan Solar Observatory Site

Artem Shikhovtsev [1,*], Pavel Kovadlo [1] and Vladimir Lukin [2]

[1] Institute of Solar-Terrestrial Physics SB RAS, 126 a Lermontova st., 664033 Irkutsk , Russia
[2] V.E. Zuev Institute of Atmospheric Optics SB RAS, 1 Academician Zuev sq., 634055 Tomsk, Russia
* Correspondence: Ashikhovtsev@iszf.irk.ru; Tel.: +7-(3952)-428265

Received: 23 July 2019; Accepted: 24 August 2019; Published: 27 August 2019

Abstract: The paper focuses on the development of the method to estimate the mean characteristics of the atmospheric turbulence. Using an approach based on the shape of the energy spectrum of atmospheric turbulence over a wide range of spatial and temporal scales, the vertical profiles of optical turbulence are calculated. The temporal variability of the vertical profiles of turbulence under different low-frequency atmospheric disturbances is considered.

Keywords: turbulence; telescope; vertical profiles; adaptive optics

1. Introduction

The efficiency of a number of astronomical instruments depends on the integral quantities of atmospheric turbulence and on the vertical distribution of the characteristics of turbulent fluctuations of wind speed and air refractive index. Ground-based astronomical telescopes are equipped with adaptive optics systems to achieve the diffraction-limited images. The development of modern adaptive optics systems to correct the optical distortions in a few planes of optical conjugation requires information on the turbulence in individual atmospheric layers, its thickness and heights. The design of a multiconjugated adaptive optics systems should be based on the simulation of light propagation in the turbulent atmosphere. To simulate, one needs to know the vertical profiles of wind speed $V(z)$ and the structure constant of the air refractive index fluctuations $C_n^2(z)$ estimated for long time intervals. The vertical turbulence profiles ($V(z)$ and $C_n^2(z)$) make it possible to determine the statistics affecting the quality of the astronomical images as well as estimate residual errors for corrected wavefront.

There are methods to estimate the vertical profiles of the characteristics of the optical turbulence. These methods include the measurements of turbulent characteristics (turbulent fluctuations of the air temperature and wind speed) or development of approaches to parameterize the optical turbulence [1–4]. To estimate turbulent characteristics, models based on calculations of vertical gradients of wind speed and air temperature are used. In this case, the distance between the nodes along the vertical direction is often large. For example, the approach based on vertical gradients of air temperature and wind speed as well as the outer scale of turbulence can be used for mid-latitudes. Despite numerous attempts to describe the global distribution of the Fried radius (or seeing), it is obvious that, in the equatorial region, such method to calculate the characteristics of optical turbulence does not work. Namely, the calculated values (seeing) are an order of magnitude lower than those observed [5].

The paper considers the problem of determination of the vertical profiles of the turbulent characteristics averaged over long time intervals (∼several years) using the spectral method. The basis

of the spectral method is the stability of the shape of a statistically averaged (over an ensemble of states) energy spectrum of atmospheric turbulence in a wide range of spatial and temporal scales.

It is known that the formation of large-scale (synoptic) inhomogeneities often observed in the earth's atmosphere is due to the development of the baroclinic instability mechanism. The proposed energy exchange schemes between different spectral ranges, as well as measurement data of vertical shifts of the horizontal component of wind speed, indicate a significant contribution of the "baroclinic" source to the formation of micrometeorological turbulence. With knowledge of the shape of the spectrum as well as the dependence of the spectral density of turbulent fluctuations on the frequency in different ranges, one can estimate the average energy characteristics of turbulence at different altitudes using the amplitudes of low-frequency atmospheric disturbances.

2. Data and Method to Estimate the Average Energy Characteristics of Turbulence Using the Amplitudes of Low-Frequency Atmospheric Disturbances

To recover the vertical $C_n^2(z)$ profiles, we use reanalysis data. There are several global datasets with medium spatial and temporal resolution to compensate the lack of direct measurements for the selected region. The wide used datasets are NCEP/NCAR (National Center for Enviromental Prediction/National Center for Atmospheric Research), NCEP/DOE, ERA-15, ERA-40 and ERA-Interim. The differences between the datasets are small, but can be significant when analyzing small changes in the meteorological characteristics.

To calculate the characteristics of the low-frequency atmospheric disturbances, we have used air temperature data from the NCEP/NCAR reanalysis data set, which is the result of assimilation of measurement data. The data assimilation system uses a 3D-variational analysis scheme, with 28 sigma levels in the vertical and a triangular truncation of 62 waves, which corresponds to a horizontal resolution of approximately 200 km [6]. The NCEP/NCAR dataset covers the period from 1948 to the present, and data are available every 6 h or four times per day (12:00 a.m., 6:00 a.m., 12:00 p.m. and 6:00 p.m. UTC). At the Sayan Solar Observatory site, the air temperature values at 17 isobaric levels (1000, 925, 850, 700, 600, 500, 400, 300, 250, 200, 150, 100, 70, 50, 30, 20, 10 hPa) have been used. To estimate the average energy characteristics of the low-frequency atmospheric disturbances, we have chosen the region limited by 50 N from the south, 52.5 N from the north and 100 E from the west, and 102.5 E from the east.

According to [7], we have calculated the air temperature dispersions in the spectral range from $8.3 \times 10^{-3}\, 1/h$ to $4.2 \times 10^{-2}\, 1/h$ for different altitudes in the atmosphere. The calculated values of the air temperature dispersions correspond to the spectral range of large atmospheric inhomogeneities generated due to the baroclinic instability mechanism.

In the free atmosphere, the structure constant of the air refraction index fluctuations C_n^2 has been calculated using the following formula based on the energy spectrum [7,8]:

$$C_n^2(z) = \left(\frac{AP(z)}{< T >^2 (z)}\right)^2 \cdot \frac{E(f_L, z) exp\left(-3\left(ln\frac{f_t}{f_L}\right) - \frac{5}{3}\left(ln\frac{f_l}{f_t}\right)\right)}{0.125} \cdot f_l^{5/3}, \quad (1)$$

where $A = 80 \times 10^{-60}/hPa$, P is the atmospheric pressure, $< T >$ is the averaged air temperature, f_L is the low frequency in the synoptic range, f_t is the transition frequency from the spectrum slope "-3" to "$-5/3$", and f_l is the high frequency in the micrometeorological range. The power spectral density of the air temperature fluctuations $E(f_L, z)$ is determined by the formula [7]:

$$E(f_L, z) = \frac{a(f_t, f_L)\sigma_T^2(\tau)}{f_L}, \quad (2)$$

where coefficient of proportionality $a(f_t, f_L) \sim 0.3$, and the air temperature dispersions are calculated from the detrended time series of the air temperature. This approach gives underestimated values of the isoplanatic angle. In order to take into account the changes in the spectrum slope in the transition region between the mesoscale interval and the range of small-scale turbulence, we suggest using a new expression to calculate $C_n^2(z)$:

$$C_n^2(z) = \left(\frac{AP(z)}{< T >^2 (z)}\right)^2 \cdot \frac{E(f_L, z) exp\left(-3\left(ln\frac{f_t}{f_L} + ln\frac{f_tm}{f_tL}\right) - \frac{5}{3}\left(ln\frac{f_l}{f_tm} + ln\frac{f_tm}{f_t}\right)\right)}{0.125} \cdot f_l^{5/3}, \quad (3)$$

where f_t is frequency of transition from "-3" spectrum slope in the synoptic range to "$-5/3$" slope in the mesoscales, and f_{tm} and f_{tL} are the frequencies in the transition micrometeorological region. The obtained formula is based on the approach [7] and refined shape of the turbulence spectrum (Figure 1). Schematically, the frequencies of the energy spectrum used in the modification of the spectral method are shown in Figure 1. PSD is the power spectral density of the turbulent fluctuations. Figure 1 is the result of the generalization of the turbulence spectrum including synoptic scales, mesoscales, transitional interval, and micrometeorological range [7,8].

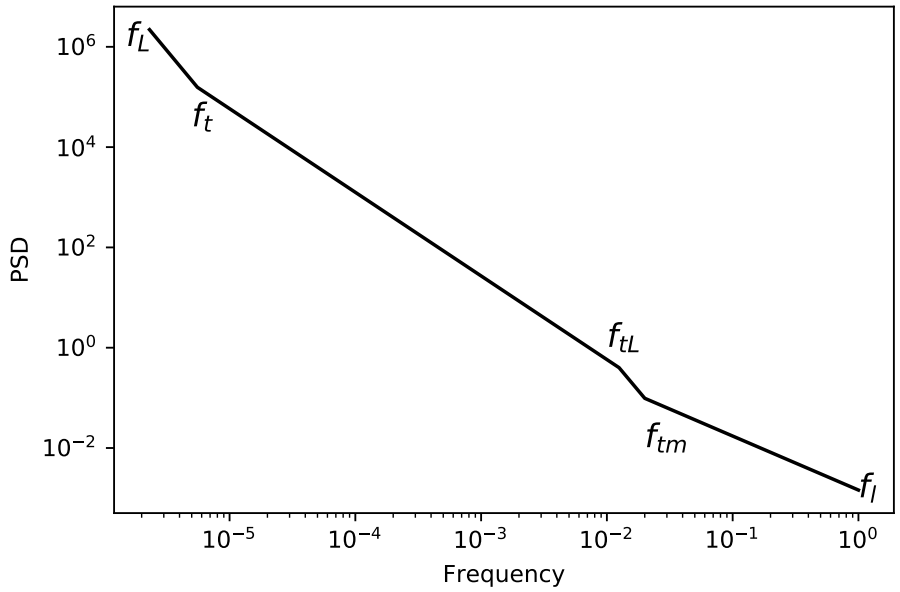

Figure 1. The scheme of the energy spectrum of the atmospheric turbulent flow. The frequencies are shown by f_L,f_t,f_{tL},f_{tm}, f_l. The dimensionless frequencies and power spectral density of the air temperature fluctuations are shown along the horizontal and vertical axes (in logarithmic scales).

The use of the dependence of the power spectral density on the frequency f^{-3} is based on the results of the analysis of measurement data [8]. It has been shown that energy of the turbulence is significantly reduced in the transition range of scales (from $\sim$ 60 m to $\sim$ 600 m) [8].

3. Results

Using Equation (3), the averaged structure constants of the air refractive index fluctuations on the standard isobaric surfaces have been calculated from reanalysis data. The constants C_n^2 on the standard isobaric surfaces have been calculated for three regimes: weak turbulence ($r_0 = 8.3$ cm), moderate turbulence ($r_0 = 4.5$ cm) and strong turbulence ($r_0 = 3.3$ cm, $r_0 = 3.8$ cm). Figure 2 shows the

averaged vertical profiles of the structure constant of the air refraction index fluctuations in conditions of weak turbulence ($r_0 = 8.3$ cm), moderate turbulence ($r_0 = 4.5$ cm) and strong turbulence ($r_0 = 3.3$ cm, $r_0 = 3.5$ cm) at the Sayan solar observatory site. The horizontal axis represents the altitudes above the observatory level and the vertical axis represents C_n^2 values in logarithmic scale. The vertical profiles are averaged for the period from 1 January 1988 to 31 December 2018.

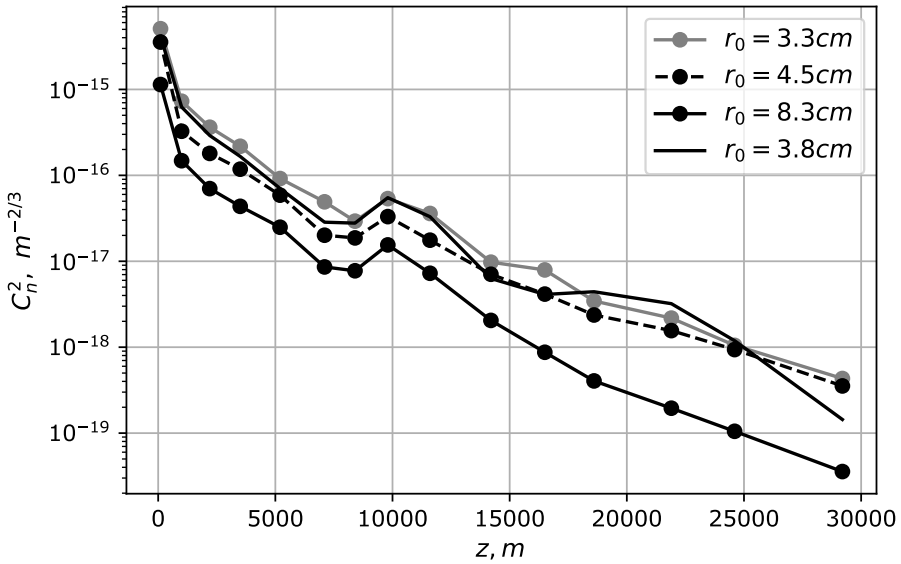

Figure 2. The vertical profiles of the structure constant of the air refraction index fluctuations at the Sayan solar observatory site. The vertical profiles correspond to different intensities of the atmospheric turbulence along light of sight.

In the atmospheric surface layer, the values of C_n^2 were calculated from measurements using an automatic meteorological system. Fried radius values for selected atmospheric conditions have been estimated using the Equation (4):

$$r_0 = \left(0.423 k^2 sec\alpha \int_0^H C_n^2(z) dz \right)^{-3/5}, \quad (4)$$

where α is the zenith angle, $k = 2\pi/\lambda$, λ is the wavelength of the light, and H is the height of the upper boundary of the "optically active" atmosphere. Calculations are performed for $\lambda = 0.5$ μm. Large values of the Fried radius correspond to the low intensity of the turbulence, and vice versa.

Analysis of the vertical changes in the optical turbulence at the site of the Sayan Solar Observatory shows that the energy constant C_n^2 decreases with height. The most developed turbulence is observed in the atmospheric boundary layer, and averaged values of C_n^2 vary from 5×10^{-16} m$^{-2/3}$ to 8×10^{-15} m$^{-2/3}$ (individual values may differ by more than an order of magnitude). In addition, an atmospheric layer with intense turbulence is observed in the vertical profiles obtained for different atmospheric conditions at a height of about 10 km above the astronomical observatory. It can also be noted that deformations of vertical profiles at the individual heights are often observed under conditions of intense atmospheric turbulence along the line of sight (with decreasing Fried radius). This may be due to the peculiarities of the development of turbulence as well as mountain waves in complex relief.

The obtained vertical profiles C_n^2 are in agreement with the data of direct optical measurements at the site of the Sayan solar observatory. The calculated averaged values of the Fried radius for the nighttime from the measurements of the differential monitor of image motion, as well as measurements of image motion in the daytime in the optical scheme of the Automated Solar Telescope are consistent with the spectral estimates obtained in this paper.

In addition, the plausibility of vertical profiles is confirmed by estimates of the isoplanatic angles calculated by the formula [9]:

$$\theta_0 = \left(2.91 \left(\frac{2\pi}{\lambda} \right)^2 \sec^{8/3} \alpha \int_0^H C_n^2(z) z^{5/3} dz \right)^{-3/5}, \quad (5)$$

where α is the zenith angle, z is the height, λ is the light wavelength, and H is the height of the upper boundary of the "optically active" atmosphere. The values of θ_0 are very sensitive to turbulence in the upper layers of the "optically active" atmosphere ($z^{5/3}$). Small deviations in C_n^2 estimates in the upper layers can lead to a change of the isoplanatic angle by several arc sec. At the same time, the calculated values of averaged isoplanatic angle are 0.82, 0.92, 1.09, 2.10 arc sec for r_0 = 3.3, 3.8, 4.5, 8.3 cm, respectively.

4. Conclusions

The spectral method to calculate the characteristics of the optical turbulence by the amplitudes of low-frequency variations of the air temperature has been improved. The method allows for estimating the values of the structure constant of the air refraction index fluctuations more accurately: the calculated values of the isoplanatic angle by the spectral method are close to the values estimated from the images (∼1.0–2.0 arc sec). The calculated values of isoplanatic angle are 0.82, 0.92, 1.09, 2.10 arc sec for r_0 = 3.3, 3.8, 4.5, 8.3 cm, respectively.

Although the method takes into account wind speed when estimating the scale f_L [7], the wind regime can affect the accuracy of the estimates. This effect is due to deformations of the spectra of the fluctuations of the air temperature and wind speed under different atmospheric conditions. In the paper, we took into account that the slope of the energy spectrum in the free atmosphere changes in the spectral range from ∼60 m to ∼600 m [8]. Taking into account this range, we estimate the spectral power density of small-scale fluctuations more accurately (by 20–30%).

Vertical profiles of C_n^2 have been obtained at the site of the Sayan solar observatory for a different Fried radius. The vertical profile for $r_0 = 8$ cm can be used to optimize both classical adaptive optics systems and multi-conjugated systems for image correction under good astrooptic conditions when the adaptation efficiency is maximum.

Author Contributions: P.K. and A.S. equally participated in the development of the spectral method. A.S. performed the calculations of the vertical profile of the optical turbulence. V.L. provided a comparison of calculated data with measurements. All authors contributed equally to this work.

Funding: This research was funded by RSF grant "19-79-00061".

Acknowledgments: Verification of the results was performed using the Unique Research Facility Large Solar Vacuum Telescope under FR program II.16.

Conflicts of Interest: The authors declare no conflict of interest.

References

1. Bounhir, A.; Benkhaldoun, Z.; Carrasco, E.; Sarazin, M. High-altitude wind velocity at Oukaimeden observatory. *MNRAS* **2009**, *398*, 862–872. [CrossRef]

2. Giordano, C.; Vernin, J.; Vázquez Ramió, H.; Munoz-Tunon, C.; Varela, A.M.; Trinquet, H. Atmospheric and seeing forecast: WRF model validation with in situ measurements at ORM. *MNRAS* **2013**, *137*, 3102–3111. [CrossRef]
3. Hagelin, S.; Masciadri, E.; Lascaux, F. Wind speed vertical distribution at Mt Graham. *Mon. Not. R. Astron. Soc.* **2010**, *407*, 2230–2240. [CrossRef]
4. Masciadri, E.; Vernin, J.; Bougeault, P. Bougeault 3D mapping of optical turbulence using an atmospheric numerical model. *Astron. Astrophys. Suppl. Ser.* **1999**, *137*, 185–202. [CrossRef]
5. Osborn, J.; Sarazin, M. Atmospheric turbulence forecasting with a General Circulation Model for Cerro Paranal. *MNRAS* **2018**, *480*, 1278–1299. [CrossRef]
6. Mooney, P.A.; Mulligan, F.J.; Fealy, R. Fealy Comparison of ERA-40, ERA-Interim and NCEP/NCAR reanalysis data with observed surface air temperatures over Ireland. *Int. J. Climatol.* **2011**, *31*, 545–557. [CrossRef]
7. Kovadlo, P.G.; Lukin, V.P.; Shikhovtsev, A.Y. Development of the model of turbulent atmosphere at the Large solar vacuum telescope site as applied to image adaptation. *Atmos. Ocean. Opt.* **2019**, *32*, 202–206. [CrossRef]
8. Vinichenko, N.K.; Pinus, N.Z.; Smeter, S.M.; Shur, G.N. The spectrum of turbulence in thermally stratified atmosphere. In *Turbulence in the Free Atmosphere*; Rusakova, G.Y., Ed.; Gydrometeoizdat: Leningrad, Russia, 1976; pp. 286–300.
9. Hickson, P. *Fundamentals of Atmospheric and Adaptive Optics*; The University of British Columbia: Vancouver, BC, Canada, 2008; pp. 1–68.

© 2019 by the authors. Licensee MDPI, Basel, Switzerland. This article is an open access article distributed under the terms and conditions of the Creative Commons Attribution (CC BY) license (http://creativecommons.org/licenses/by/4.0/).